CHAPTER 2

Introducing the oceans

Yueng-Djern Lenn[a], **Fialho Nehama**[b], **and Alberto Mavume**[b]
[a]School of Ocean Sciences, Bangor University, Menai Bridge, United Kingdom
[b]Escola Superior de Ciências Marinhas e Costeiras, Universidade Eduardo Mondlane, Quelimane, Mozambique

1. Our blue planet

The dawn of the space age not only heralded humanity's exploration beyond our planet but also provided the unprecedented opportunity to look back from afar and consider our planet and how it sustains our existence. The view of Planet Earth from space (Fig. 2.1), as immortalized by the Apollo 17 crew in 1972, brings our home into sharp focus as a beautiful blue planet against the infinite blackness of space.

Thus far, our exploration of space by manned and unmanned spacecraft, as well as with our powerful radio telescopes, has yet to locate and identify another planet so abundant in the surface waters that make our planet blue. Any oceanographer can tell you that our oceans cover over 70% of the Earth's surface and are indescribably fascinating and beautiful, but perhaps more importantly, are absolutely vital to life on Earth and the functioning of our climate system.

Many different types of water bodies exist on the surface of the Earth, from lakes fed by melting mountain snowpacks to rivers and ponds. To follow a river onwards from its source will almost inevitably lead you out to sea, to the big blue ocean that begins where the land ends. Our oceans reach from pole to pole, covering vast areas with seawater that moves in myriad ways. Not all seawater resides in liquid form; some of it is frozen into sea ice in the far north and the far south, floating on the polar seas as drifting ice packs. The oceans reach far deeper from the sea surface (down to 11 km in Challenger Deep of the Marianas Trench) than the tallest mountains rise above the sea level (Fig. 2.2). Yet paradoxically, typical depths of ocean basins are shallow (under 4 km on average, reaching 5 km at the abyssal plains) relative to their horizontal spread (spanning tens of thousands of kilometers between continents) such that the oceans are essentially a thin blue layer lying atop the Earth's crust with an aspect ratio akin to a sheet of paper.

A Journey Through Tides
https://doi.org/10.1016/B978-0-323-90851-1.00018-2

Fig. 2.1 Blue marble. View of Planet Earth from the window of Apollo 17 as photographed by the crew members in December 1972. *(Photograph from NASA.)*

Within this thin blue layer lives the oceanic ecosystem, where the seaweed and phytoplankton that perform photosynthesis in the sunlit upper ocean provide 50% of the oxygen on Earth while fixing dissolved atmospheric carbon dioxide into sugars (Friedlingstein et al., 2020). Predators that consume phytoplankton and descend to respire at depth, or death and other biological processes that result in sinking organic carbon detritus known as marine snow, in addition to physical processes like downwelling currents conspire to store, within our oceans, 50 times the carbon found on land (Friedlingstein et al., 2020). Consequently, research into ocean sequestration of atmospheric carbon dioxide and other ways in which the oceans are currently holding back the worst impacts of climate change continues unabated, and with increasing intensity in the early 21st century.

Our oceans' contribution to global carbon cycles aside, their impact on the day-to-day lives of people is equally profound. Approximately, 40% of humanity lives within 100 km of the coast (Small and Nicholls, 2003), with many depending directly on it for food, livelihoods, and recreation, and being subject to marine-mediated impacts on local weather. These coastal populations are among the fastest growing on the planet and many such

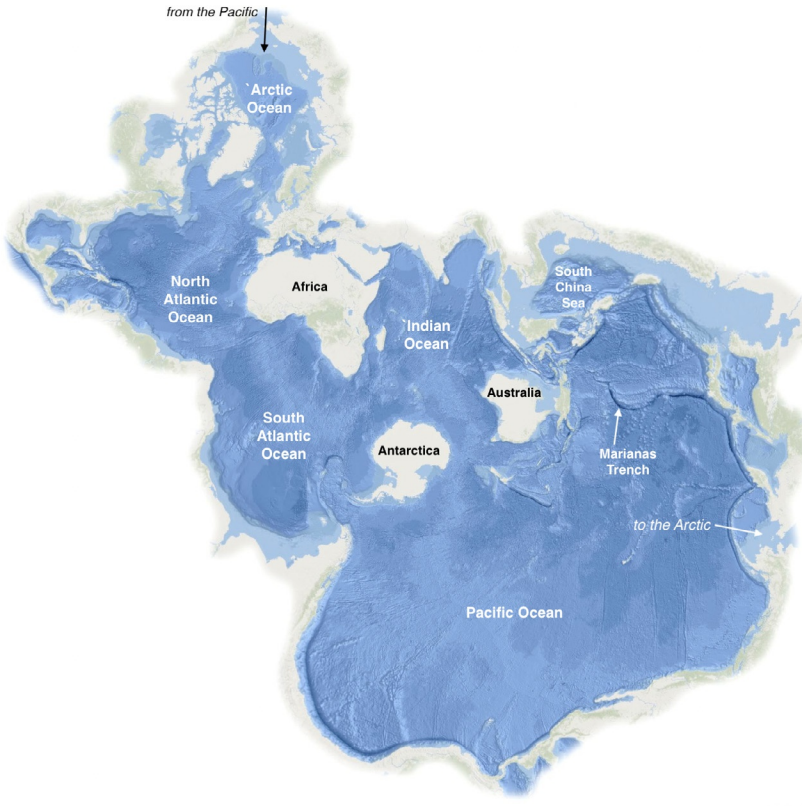

Fig. 2.2 Bathymetry of the world's ocean mapped on the Spilhaus projection. Darker blues indicate deeper waters.

populations, particularly across south and southeast Asia, face increasing vulnerability to extreme weather events such as coastal flooding exacerbated by sea level rise (Neumann et al., 2015). In addition, global commerce and our economies rely on shipping to transport goods and products across the oceans. For instance, at least 70% of all trade between Europe and other nations takes place by sea, utilizing the global shipping network that connects all the coastal nations of our globe (Hoffmann et al., 2017). The ocean's relevance to how all of us live cannot be overstated.

Because of its relative remoteness and unsuitability as an easily-settled human habitat, the sea remains a place of mystery and romance, both scientifically and literally. We have yet to truly plumb the depths to discover all there is to know about the ocean and the inhabitants of this watery realm. As Helen Scales so evocatively explains in her popular science book *The Brilliant*

Abyss (Scales, 2021), never-before-seen deep sea species continue to be discovered on every new deep ocean expedition that is mounted. Consequently, marine biologists consider our understanding to be barely scratching the surface of all there is to know about our fellow earthlings. From tales of the lost Atlantis to Jules Verne's *20,000 Leagues under the Sea* (Verne, 1869) and so on, the sea remains an infinite source of inspiration for storytellers, explorers, and scientists.

Nonetheless, there is a lot we can say about how our oceans work. We know, for instance, that our sun is the primary source of heat for our planet's surface and our oceans. We know that our atmosphere, land, and oceans absorb this solar radiation at variable rates and that the solar radiation is unequally distributed from the equator to the poles. This spatial variability in solar heating and the intrinsic rotation of the Earth together drive atmospheric circulation, which in turn forces ocean circulation. Ocean currents themselves are subject to angular momentum conservation as they flow around our rotating Earth, and from the subtropics to the poles, we experience seasonal variability that results from Earth's axis of rotation being non-normal to our orbital plane around the sun. Speaking of which, both the Sun and Moon exert a gravitational pull on our oceans that drive the tides, which are the focus of this book.

This chapter will introduce fundamental oceanography concepts that will help you understand tidal dynamics and the impact the tides have on our oceans and planet that is discussed in the other chapters. Here, we explain how seawater is characterized by its state variables like temperature and salinity and how these seawater properties tell us about ocean mixing and dynamics. We will explain how our globally interconnected ocean circulates within gyres residing within the major ocean basins, which in turn are surrounded by continental shelf seas that creep up estuaries to mix with freshwater from rivers, and how it freezes in the polar regions to float about the sea. We will consider how seawater properties act as tracers that tell us where and when any specific water parcel was last at the surface of the ocean and how these water masses spread throughout the global ocean. Finally, we will explain the ocean's role in Earth's climate system and how it mediates our weather and enables life on Earth.

2. Physical properties of seawater

Energy input to the ocean via winds or tides drives ocean currents, but ocean currents can also be driven by differences in density. In the classic lockgate

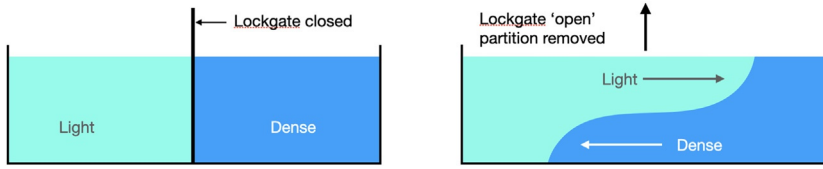

Fig. 2.3 Lockgate schematic. Left: Lockgate closed configuration with a partition separates fluids of different density. Right: partition is removed as the lockgate is "opened," allowing the dense water to flow under the light water as the water column adjusts.

experiment (Fig. 2.3), dense water is separated from lighter water in a rectangular tank by a plane barrier, representing a situation that is typical for regions of freshwater influence, but is also known to occur in open ocean when there are density gradients. When the lockgate is opened by removing the barrier, the dense water slides under the lighter water as a density current, eventually filling the bottom of the tank beneath a lighter layer. This adjustment from the initial high potential energy state to a stable two-layer minimum potential energy state is driven by the density differences between the two layers.

Seawater density (usually denoted by ρ) is not only a driving force in density currents but is also a key property to the understanding of how seawater is layered, or *stratified,* within the global ocean. Ocean stratification in turn sets the kinetic energy input required to overcome the potential energy barrier to mix different layers and their respective properties such as heat, salt, and nutrients together. The physical properties that determine seawater density are known as state variables, and these are the quantities measured by oceanographers seeking to understand ocean physics.

The state variables of seawater that set its density are temperature, T, and salinity, S. Temperature is a measure of the heat stored within the ocean and increases in heat content result in the thermal expansion of seawater, reducing its density. Salinity is a measure of the salt content of the seawater and is the counterpoint to its freshwater content. Salinity is defined as the concentration of salt (typically dissolved sodium chloride) in seawater and is given in parts per thousand by weight or grams per kilogram. Increases in salinity imply higher concentrations of dissolved salt and thus increase the density of seawater. The relative impact of changes on seawater density are given as $\Delta\rho = -\alpha\Delta T + \beta\Delta S$, where α is the coefficient of thermal expansion and β is the haline contraction coefficient, approximately equal to 0.0008. The thermal expansion coefficient is dependent on the temperature, and we do not have a simple expression for it.

The heat content that sets seawater temperature mostly comes from the Sun. Solar radiation across the visible spectrum, from the short ultraviolet/blue wavelengths to the longer red wavelengths, easily passes through the Earth's atmosphere without much absorption. When it reaches the ocean, the Sun's rays penetrate the surface ocean powering photosynthesis in marine ecosystems and illuminating the upper ocean. This radiation does not reach the seafloor of ocean basins. Indeed, the red wavelengths are quickly absorbed by, and warm, water molecules such that by about 30 m below the sea surface, blue light dominates the view. Descend much further, and soon even these short wavelengths are absorbed by the water as the ocean grows as dark as midnight. All this absorption of solar radiation warms our oceans from the top, resulting in sea surface temperatures ranging from approximately −2 °C in polar oceans to 30 °C at the equator (Fig. 2.4, lower panel). Consequently, any profiling temperature-measuring instrument dropped into the subtropical or mid-latitude ocean will register ever-decreasing temperatures as it descends (Fig. 2.5).

In addition to solar radiative fluxes, the ocean can also gain heat through conductive fluxes (e.g., hot atmosphere over cool ocean), warm river discharge into the polar oceans (Park et al., 2020), and be heated by hydrothermal vents from below (Adcroft et al., 2001). Conversely, the ocean also loses heat at the surface through conduction (sensible heat fluxes), emission of longwave infrared radiation, and latent heat fluxes associated with phase changes arising from evaporation and ice formation/melting. High winds and the breaking of wind-driven waves will tend to enhance evaporation and ocean heat loss to the atmosphere. The combined effect of these processes effectively sets the ocean temperature, which is the main determinant of ocean density changes outside of the polar oceans.

Salinity of course arises from dissolved salt put into the oceans. The total salt content of the oceans is thought to have accumulated over millennia from mineral rock salts dissolved and washed into the sea by the rain. Rainwater-dissolved mineral rock salt does continue to enter the ocean from rivers; however, these modest increases in salt content are more than offset and diluted by the freshwater input of the river water itself. As a result, the salt content of the ocean is considered to be relatively stable at ocean salinities of about 35 parts per thousand, which is found almost everywhere in the global ocean.

Nonetheless variations in ocean salinity do exist, and these variations are largely driven by the addition or removal of freshwater from the ocean. Along coastlines, freshwater input from rivers results in regions of freshwater

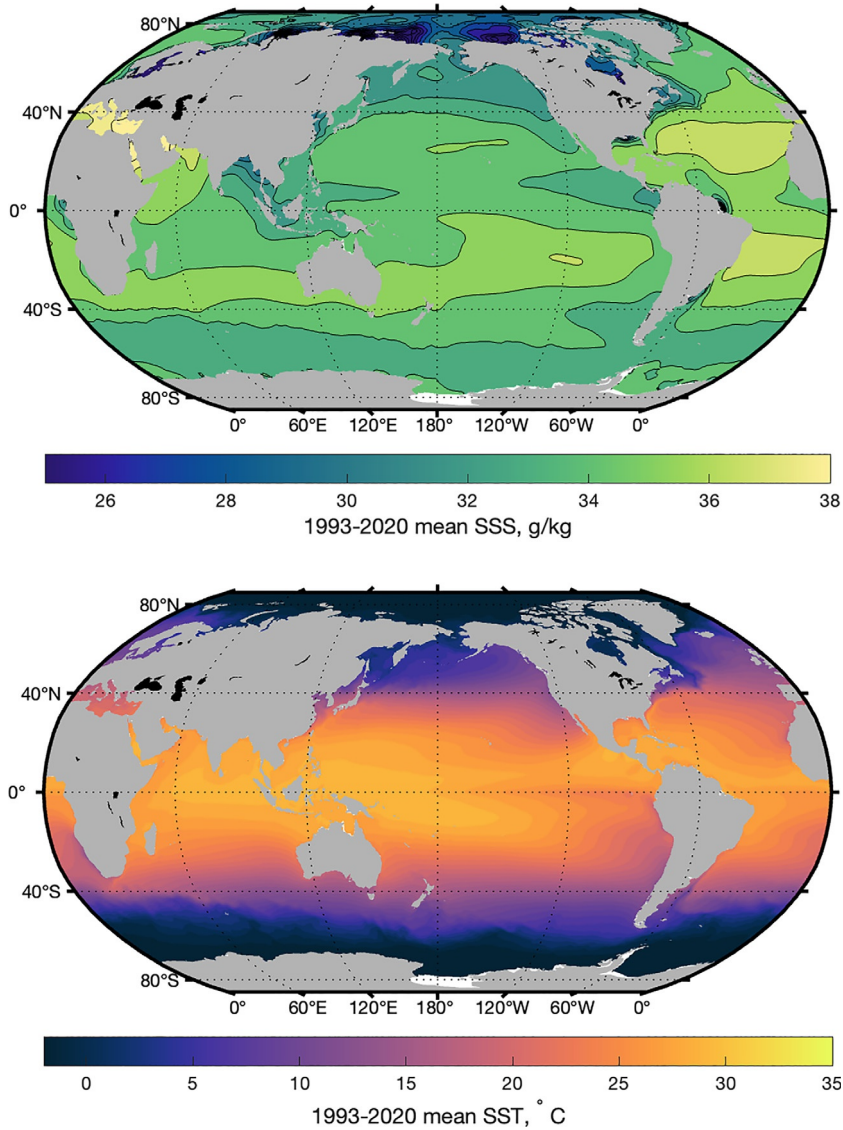

Fig. 2.4 Average sea surface salinity (upper) and sea surface temperature (lower) for the period 1930–2020, from the hydrographic ARMOR3D dataset (Guinehut et al., 2012).

influence where mainly fresh regions are separated from seawater by tidal mixing fronts (Sharples and Simpson, 1993). Farther out to sea, it was Robert Boyle who first noted that the ocean was salty from the sea surface to the seabed, and that it is the competing effects of evaporation and

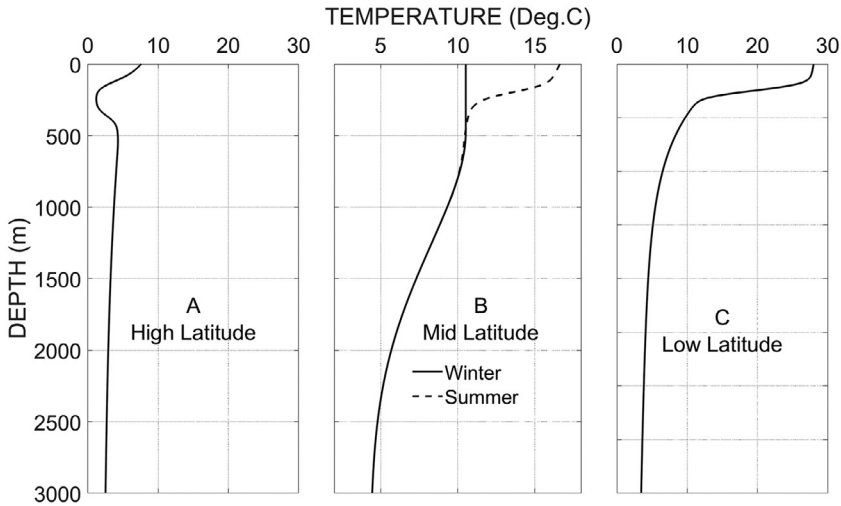

Fig. 2.5 Temperature profiles at (A) high, (B) mid, and (C) low latitudes.

precipitation that determined sea surface salinities (Boyle, 1685). Thus ocean salinity is generally higher at the surface than at depth because only the surface is subject to evaporation (Fig. 2.6). Across different latitudes, precipitation under the intertropical convergence zone and mid-latitude storm tracks, evaporation in the sunny subtropical latitudes, and sea ice and glacial

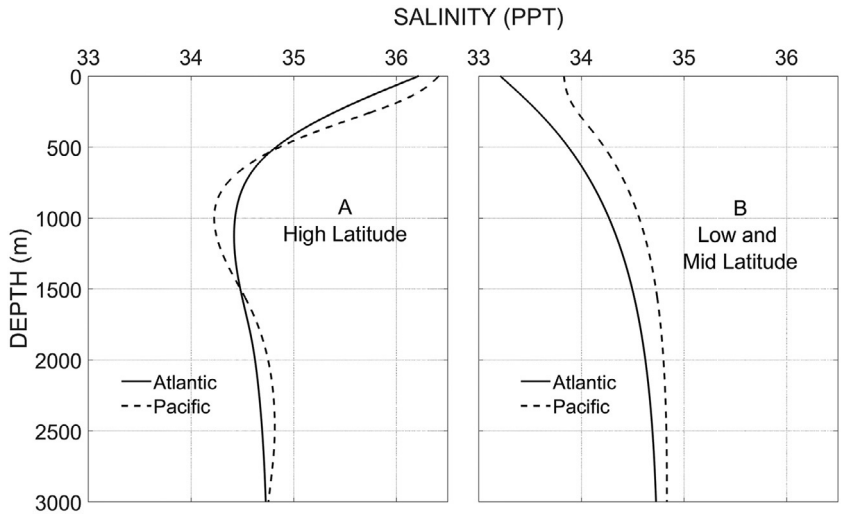

Fig. 2.6 Salinity profiles at (A) high, (B) mid, and low latitudes for the Atlantic and Pacific oceans.

melt in the polar oceans result in alternating patterns of sea surface salinity highs and lows (Fig. 2.4, upper panel). Partially because of the very small range of ocean salinities (i.e., 34–37), but mainly because of the strong dependence of density on temperature, the ocean salinity impact on density is generally minor in the global ocean. This impact is larger in semienclosed basins and estuaries and may even surpass that of the temperature.

At most latitudes, the twin effects of temperature and salinity result in a warm and often salty surface mixed layer (SML, see T-S profiles). Within the surface mixed layer, generally 50–100-m deep except in winter when the SML at high latitudes reaches the 400 m depth, wind-driven mixing and convection arising from surface buoyancy fluxes combine to thoroughly mixed heat and salt properties. Below the largely homogenous mixed layer lies, in general, the ocean thermocline. This thermocline can be several hundred meters to a km thick and is characterized by a steep vertical gradient in temperature. Where temperature effects on density dominate (i.e., most of the global ocean), the ocean thermocline functions also as its pycnocline in which steep gradients in density act as energy barriers to mixing of water properties between the layers above and below the pycnocline. Below the SML, both ocean temperatures and salinities generally decrease with depth, with the density reduction from lower salinities being greater than the offset by the contraction due to cooler temperatures. Thus the ocean is usually stably stratified with lighter waters overriding dense waters.

At very low temperatures, the salinity influence on density takes precedence over temperature. As seawater cools toward the freezing point, it contracts and its density increases until it reaches the temperature of maximum density (Fig. 2.7). For pure water, this is 3.98 °C, and for typical seawater salinities, it is approximately 0 °C. As water cools below the temperature of maximum density, liquid water expands again until it reaches the freezing point and changes phase into ice which is even less dense and floats atop the liquid water. Thus in the polar oceans, at near-zero temperatures and below, the density and the resulting stratification is set by salinity, rather than temperature. This is why, for instance, the Arctic is considered an "upside-down" ocean, where a very fresh cold surface mixed layer floats above a halocline layer, characterized by a marked vertical gradient in salinity, which in turn overrides much warmer saltier water of Atlantic origin below, a reversal of the water properties' depth profile seen at lower latitudes.

The last important state variable of seawater is its in situ pressure, P. Seawater contracts, slightly, under pressure, and within the ocean, this hydrostatic pressure is given by $P = H\rho g$, where H is the water depth and

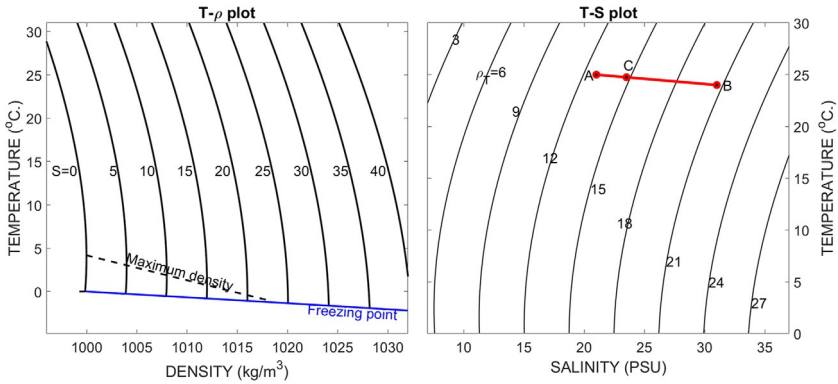

Fig. 2.7 Temperature of maximum density of seawater at $P = 1.023\ 10^5$ Pa (left) and water masses displayed on a T-S diagram (right).

g is the acceleration due to gravity. Hydrostatic pressure is isotropic causing the seawater to contract equally in all directions, such that the increased proximity of water molecules effectively increases the internal energy or heat of the water parcel under pressure. Hence, the pressure effect on temperature must be accounted for in order to be able to directly compare the temperature of water parcels at different depths. Therefore pressure, or depth by inference, is always measured alongside temperature and salinity. Historically, once the pressure effect has been accounted for, the corrected in situ temperature T is known as potential temperature, θ, which is defined as the temperature of the water parcel if it had been adiabatically moved to a reference depth, usually the surface. Using the modern standard TEOS10 (Thermodynamic Equation of State 2010, http://www.teos-10.org) Gibbs seawater routines based on the thermodynamic principles, oceanographers have adopted conservative temperature, Θ, and absolute salinity, S, as the new standard pressure-corrected hydrographic state variables.

3. Geography and ocean circulation

On World Oceans Day, June 8, 2021, the National Geographic Society acknowledged the Southern Ocean as the fifth ocean basin on our planet. The Southern Ocean joined the Atlantic, Pacific, Indian, and Arctic Oceans in recognition of its unique circulation and water properties that distinguished it from the other basins. This of course was not remotely news to oceanographers who have long considered the Southern Ocean as a major ocean basin, that yes, is unique in many respects. The Southern Ocean hosts

the mighty Antarctic Circumpolar Current (ACC) which rushes in a continuous braided eddying stream around Antarctica, connecting the Atlantic, Pacific, and Indian Oceans at high southern latitudes. The ACC is forced directly by westerly winds, which are unimpeded by land masses as they encircle the globe, and effectively separates warmer subtropical waters to the north from colder polar waters to the south (Speer et al., 2000). These winds also drive a northward surface Ekman transport that draws isopycnals (i.e., surfaces of equal density) toward the surface, making the Southern Ocean the largest upwelling region on the globe (Fig. 2.8). This upwelling brings nutrients (i.e., nitrates, phosphates, silicates) to the upper layers of the ocean and has profound consequences for water mass formation. Along with the nutrients, CO_2-enriched deep waters are vertically imported to the upper ocean, allowing them to interact with the atmosphere and impact the climate (a topic that will be discussed in the next two sections).

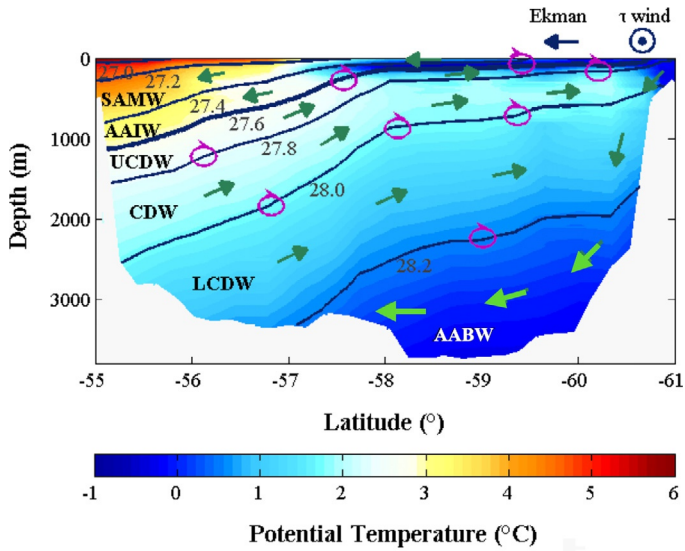

Fig. 2.8 Southern Ocean upwelling and downwelling indicated by green arrows against a background of potential temperature. Upper and lower circumpolar deep water (UCDW, CDW, LCDW) upwell along isopycnals, while Antarctic Bottom Water (AABW) cascades down the continental slope to the abyss. Subantarctic mode water (SAMW) and Antarctic Intermediate Water (AAIW) are carried north by the wind-driven Ekman transport and subduct below the subtropical mode waters to the north. *(Modified with permission from Silvester, M.J., Lenn, Y.D., Polton, J., Rippeth, T. P., Morales Maqueda, M. 2014. Observations of a diapycnal shortcut to adiabatic upwelling of Antarctic Circumpolar Deep Water. Geophys. Res. Lett. 41, 7950–7956.)*

Winds are also responsible for driving the circulation of the five major subtropical ocean gyres. These gyres occupy the 4–5-km-deep basins of the North and South Atlantic, the North and South Pacific, and the Indian Oceans. Moving either north or southward away from the equator, the prevailing wind direction switches from the easterly trade winds blowing along the equator to westerly winds as latitude increases. This divergence in the zonal wind stress drives a surface Ekman convergence, piling water into the center of each subtropical gyre, and depressing the thermocline (Fig. 2.9). Ocean dynamics within subtropical gyres are dominated by the Sverdrup balance between the Earth's rotation and wind stress, such that the depth-integrated meridional basin transport V is given by

$$\beta V = \mathbf{k} \cdot \nabla \times \tau \tag{1}$$

where β is the meridional gradient of the Coriolis parameter f, $\mathbf{k}$ is the unit vector in the z (vertical) direction, and τ is the surface wind stress

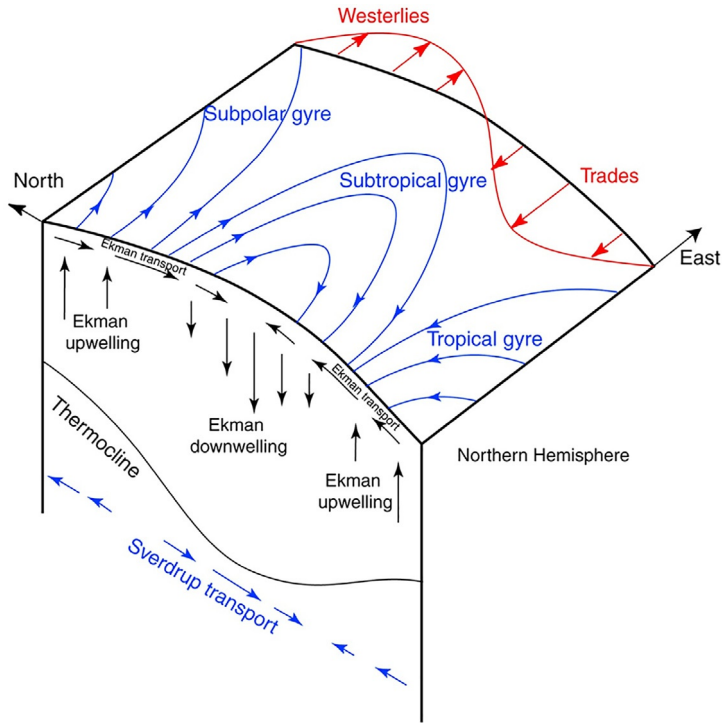

Fig. 2.9 Sverdrup gyre cross-section, reproduced from Talley et al. (2011). Wind stress (*red arrows*) drive a basin-scale horizontal circulation (*blue arrows*) and Ekman transports (*black arrows*) that result in a depressed thermocline in the middle of subtropical gyres.

(Sverdrup, 1947). This broad equatorward flow across most of the subtropical gyres effectively loses planetary vorticity as it nears the equator. To balance the mass redistribution of this southward flow, seawater must be returned polewards in narrow, intensified western boundary currents where vorticity is gained as a result of the coastal friction onshore imposing a zonal velocity gradient on the currents (Stommel, 1948). Within these western boundary currents, current speeds can reach up to $1\,m\,s^{-1}$. The key western boundary currents are the Gulf Stream and Brazil Current in the Atlantic, the Agulhas Current of the Indian Ocean, and the Kurushio and East Australian Currents of the Pacific. Poleward transport of warm salty waters in these western boundary currents vary from the ~10 Sv of the Brazil Current (Stramma et al., 1990) to the ~75 Sv of the mighty Agulhas Current (Beal and Bryden, 1999). Away from western boundaries, ocean currents within the central gyres tend to be much smaller, typically a few $cm\ s^{-1}$. These recirculating subtropical gyres are key components of global ocean circulation in which the western boundary currents, in particular the Gulf Stream of the North Atlantic, play an outsized role in the transport of ocean heat and salt away from the equator.

When tides traverse the deep ocean basins, their propagation speeds add to the ambient gyre circulation. However, over the deep basins, the tidal gravitational pull of the barotropic tide is spread out over the full water column resulting in very modest tidal currents of a few $cm\,s^{-1}$. The same gravitational pull exerted over the much shallower continental shelf seas will result in much bigger tidal currents, sometimes exceeding $50\,cm\,s^{-1}$ in places such as the Patagonian shelf (Glorioso and Simpson, 1994) or $100\,cm\,s^{-1}$ on the European shelf. Continental shelf seas mark the transition zone from the deep ocean basins to land and may be up to 4–500 m deep, although most shelf seas are closer to 100-m deep. Continental shelf seas are themselves separated from the deep ocean basins by continental shelf breaks, where the seabed typically slopes very steeply away from shore. Continental shelf breaks are energetic regions in which strong, generally narrow along-slope currents (Huthnance, 1984) act as barriers dividing the basin waters from the shelf waters. Potential vorticity constraints associated with changes in the water column thickness also conspire to limit shelf-basin exchange. Yet, shelf breaks are known to be active mixing regions where internal tides break and dissipate their energy and bed friction increases rapidly onshore (Chapter 5).

Up on the shallow continental shelf seas themselves, kinetic energy input by winds dissipated at the base of a mixed layer effectively mixes much of the

water column than in the deep ocean. Both wind and tidal energy input can be dissipated either by shear-driven mixing at the base of seasonal summer mixed layers (Rippeth, 2005) or bottom friction (Simpson et al., 1996). Winter cooling of surface waters increases their density, destabilizing the water column, driving convection that contributes to the mixing from winds and tides. Consequently, in the winter, continental shelf seas are typically characterized by homogeneous water columns, whereas warming in spring and summer leads to the development of a warm surface mixed layer that persists into early fall. The development of seasonal stratification and the wind and tide-driven mixing across the continental shelf seas have two distinct and noteworthy impacts. On one hand, mixing allows the productive surface mixed layer to be frequently supplied with deep nutrients required to sustain primary productivity. And, on the other hand, the summer stratification assures that carbon exported below the seasonal thermocline in the forms of organic detritus or respiration is effectively separated from the surface and can be deposited on the seabed or exported off the shelf into the deep ocean basins. As a result, continental shelf seas which cover only about 7% of the globe, account for 20%–50% of the organic carbon stored by the global ocean (Thomas et al., 2004; Tsunogai et al., 1999). The productivity of continental shelf seas also supports rich ecosystems that provide vital commercial and nutrition resources for coastal communities.

Tides propagating across continental shelf seas certainly do more than drive vertical mixing, and Chapter 11 will explore their impact on coasts in greater detail. For now, it is useful to know that asymmetries in tidal currents or interactions with topography can drive residual currents that contribute to the background circulation in a shelf sea (Polton, 2015). Tides are also critical in dispersing freshwater from rivers across the continental shelf beyond the estuary from which they emerge (Simpson et al., 1990). Estuaries are the regions in which the riverine freshwater first encounters seawater. In most estuaries, salty seawater sneaks landwards below the fresh and much lighter layer of river water heading out to sea (Fig. 2.10), creating a two-layer circulation that ebbs and flows with the tide (Knudsen, 1900).

The dynamic balance of the two-layer estuarine circulation depends on physical factors such as river discharge, the salinity difference between the river and seawater, lateral salinity gradients, and geographical factors such as channel breadth and depth (Pritchard, 1956). In some instances, instead of the continental shelf sea exchanging saltwater for fresh in an estuary, we have the reverse exchange. This usually occurs where the river input is negligible relative to the high evaporation taking place within these

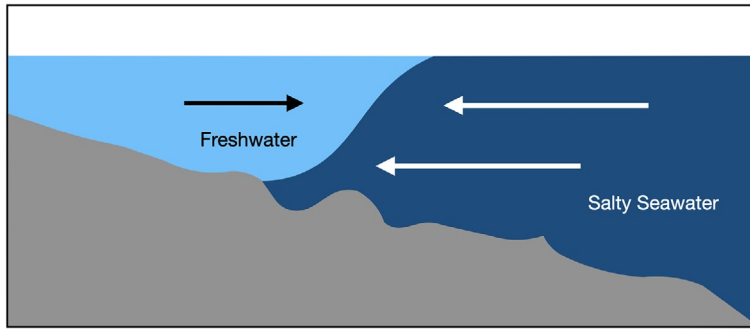

Fig. 2.10 In an estuarine salt wedge, freshwater runs atop saline water.

"*reverse estuaries*." Seawater entering reverse estuaries such as Spencer Gulf, South Australia, and the Mediterranean Sea, are subject to high evaporation on their circuit through the reverse estuary and lose buoyancy before exiting as an even saltier dense overflow below the incoming, comparatively fresher seawater (Fig. 2.11).

Freshwater also plays an important role in the dynamics of the polar seas. Antarctic sources of freshwater stem from the glaciers and ice sheets extending out into the ocean. Large icebergs that break off from the glaciers or ice sheets can be advected far out to sea where they melt slowly releasing not just the freshwater that can exceed local precipitation-minus-evaporation fluxes (Silva et al., 2006) but also all the minerals and rocks entrained into the ice as the glacier scoured its bed on route to sea (Raiswell et al., 2008). In the far North, Arctic rivers drain vast areas that are home to 40 million people and input 11% of total global riverine freshwater input into approximately 4% of the area covered by oceans (Lammers et al., 2001), making this region the freshest ocean on the planet (Fig. 2.11). Small Arctic glaciers also contribute to the Arctic freshwater budget. All this freshwater insulates the warmer saltier waters below from the atmosphere, limiting the air-sea fluxes between the warm waters of Atlantic and Pacific origin and the atmosphere.

In both polar regions, the seasonal cycle in sea ice formation and melting also exerts a big influence on the ocean dynamics. In winter, as seawater begins to freeze, it expels approximately 60% of its salt (Lake and Lewis, 1970). This process is known as brine rejection, in which near-freezing point high salinity water is fluxed into the water column below as freeze onset sets in. Brines continue to drain out of the predominantly fresh sea ice matrix throughout its lifespan (Niedrauer and Martin, 1979). Sea ice itself, particularly when consolidated into a drifting ice pack at 100%

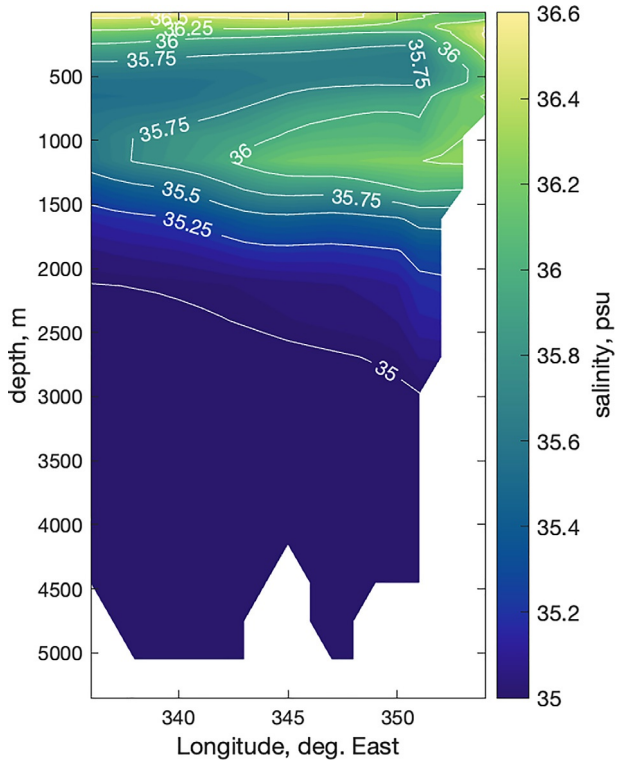

Fig. 2.11 Zonal section along 36 N with the Strait of Gibraltar to the right of the figure. Note that the high-salinity plume extends westward at ~1000-m depth, indicating the presence of the Mediterranean Overflow Water (MOW).

concentration, acts as a barrier to fluxes of heat, freshwater, and momentum between the atmosphere and ocean (Green and Schmittner, 2015). In summer, when the sea ice melts after drifting around the ocean to places usually far removed from where it froze in the first place, the meltwater forms a freshwater cap over the ocean below.

Spatial variability in the ocean stratification will have consequences on how the oceans respond to the surface wind stresses. Even though convection and two-layer exchange flows are mediated by density differences, it is still the wind that largely sets the basin-scale circulation patterns of the oceans. Beyond the five subtropical gyres (Fig. 2.12), smaller basins such as the subpolar Labrador Sea, Weddell Sea, and the Arctic Beaufort Gyre all feature their own wind-driven gyre circulations, while river plumes on

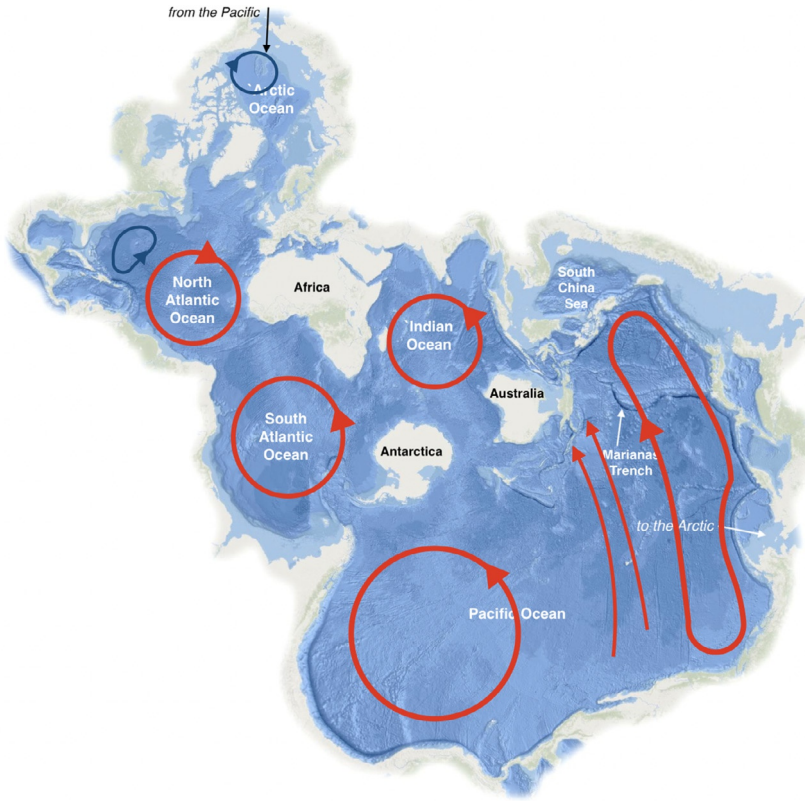

Fig. 2.12 Schematic of the five gyres of the North and South Pacific, North and South Atlantic, and Indian Ocean are shown in red. The subpolar Labrador Sea circulation and polar Arctic Beaufort gyre are also shown in *dark blue*.

continental shelves are subject to the competing effects of the winds, conservation of vorticity, and tidal straining (Horner-Devine et al., 2015; Nehama and Reason, 2021).

4. Key water masses and global distributions

As we have already seen, denser heavier water will slide beneath water that is lighter, more buoyant. In the ocean, this results in a layering of water of different densities that we refer to as stratification. It turns out that each layer, or *water mass*, has a distinct combination of temperatures and salinities that were set when it was last in contact with the surface. The process of surface properties reaching the deep ocean is known as ocean ventilation. Generally

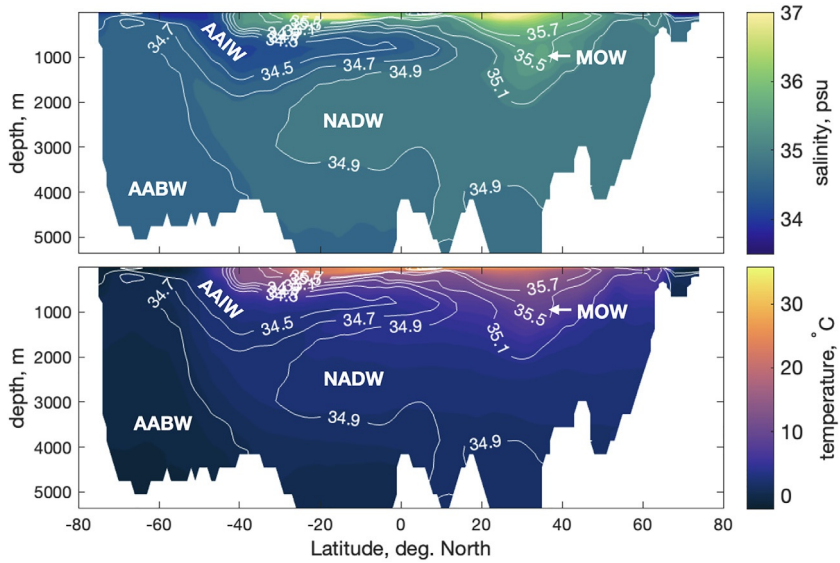

Fig. 2.13 Monthly mean meridional section along 25 W in the Atlantic Ocean for August 2020, plotted from the EN4 hydrographic dataset (Good et al., 2013). Salinity (top) and temperature (bottom) are overlaid with salinity contours in white. AABW, Antarctic Intermediate Water (AAIW), North Atlantic Deep Water (NADW), and MOW are indicated.

speaking, temperature and salinity can be used to track water masses as they are dispersed across the globe from their formation regions (Fig. 2.13). This section describes the major water masses involved in global circulation of our oceans.

Clearly, the temperature, salinity, and density of a water mass will depend on where on the planet it was formed. In the middle of subtropical gyres, solar heating and evaporation result in warm salty subtropical surface mixed layers. Solar heating peaks in the summer following which, winter cooling driving convection and storms will result in mixing of the surface waters with cooler waters below. Within the subtropical gyres, this results in a thick layer of subtropical *mode water* (STMW) of near-homogeneous temperature and density. In the Atlantic, this is commonly referred to as 18° water, a phrase originally coined to describe the mode waters of the Sargasso Sea (Worthington, 1958). STMW subduct below the warmer surface mixed layer, separating it from the ocean thermocline below, as they circulate around the gyres. Near surface, widely spaced isotherms (constant temperature contours) or isopycnals (constant density contours) on ocean cross-sections indicate the presence of mode waters.

Another water mass known for its high salt content is MOW (Mediterranean outflow water; Fig. 2.13 and see also Fig. 2.11). As

freshwater in the inflowing water from the North Atlantic is removed by evaporation within the Mediterranean basins, its salinity increases as does its density. This Mediterranean water then overflows into the North Atlantic basin through the Straits of Gibraltar below the Atlantic inflow, sinking down the continental slope in a turbulent plume and entraining ambient fresher North Atlantic water until it settles at about 1000 m depth. At this depth, the water of MOW origin is observed as a prominent subsurface salinity maximum as it spreads northwest along the European continental slope (Reid, 1979). This salty MOW-origin water ultimately mixes with other fresher colder overflows of Arctic and Nordic seas origin as it spreads west, eventually mixing with water of Labrador Sea origin densified by very deep convection (Clarke and Gascard, 1983; Lilly et al., 1999). During this transit across the subpolar North Atlantic basins, these water masses mix with each other at depth eventually creating NADW. The high salt content of NADW allows it to retain more heat than most other water masses found at this depth. NADW is exported south as a deep western boundary current in the Atlantic, eventually reaching the Southern Ocean, where the ACC redistributes it into the Indian and Pacific Oceans. South of the ACC, winds drive upwelling of NADW to the surface where this water mass is known as circumpolar deep water (CDW).

The very deep convection that has been observed in the Labrador and Nordic Seas reaches depths of around 1000 m as a result of intense winter cooling, but only over very localized areas 100 s of meters wide (Schott et al., 1994). On basin scales, winter convection in the subpolar seas deepens the mixed layers, with the deepening allowing seasonal shoaling of isopycnals (surfaces of constant density) within or immediately adjacent to the North Atlantic Current and the major boundary currents of the subpolar North Atlantic (McCartney and Talley, 1982). Within the deep mixed layers coinciding with the outcropping isopycnals, the properties of subpolar mode waters are set at temperatures in the 8–12 °C range (McCartney and Talley, 1982). Once formed, these subpolar mode waters spread through the upper ocean following the subpolar gyre circulation, with some portion being entrained into the deeper flows joining the deep western boundary current heading south.

With the coldest air temperatures and the most extreme seasons, the polar regions are key regions of air-sea heat fluxes leading to water mass formation. In the seasonally sea-ice-covered oceans, there is a seasonal cycle in dense water formation associated with the freeze-up. Seawater loses heat to the atmosphere as it cools, increasing its density. As seawater begins to freeze, approximately 60% of its salt content is rejected and released to the water

column below as dense, cold brines, with the remaining salt trapped in brine channels within the sea ice matrix that slowly continues to drain out over time (Lake and Lewis, 1970; Wettlaufer et al., 1997). These dense brines then sink through the water column, mixing with the ambient water until they reach a depth where they are neutrally buoyant. In coastal polynyas, areas where winds blown newly formed ice away from coastline, sea ice can continually form allowing the accumulation of the dense brines on the continental shelf below, creating high salinity shelf waters (Grumbine, 1991; Jacobs et al., 1979; Schauer, 1995). These high-salinity shelf waters are exported off the shelves, sinking as density currents down the continental slope. The sinking high-salinity shelf waters mix with and entrain fresher water masses forming *bottom waters* that fill up our abyssal oceans. The unintuitive thing about bottom waters is that, despite having origins in high-salinity shelf waters, they tend to be freshest water masses of their density class because of their extreme cold temperatures.

Arctic intermediate and bottom waters circulate within the Arctic basins, and some portion is exported south into the Nordic Seas in the East Greenland Current (Rudels et al., 2005). This water is further transformed on its passage through the Greenland Sea until it spills over Greenland-Scotland ridge as the Denmark Strait overflow – the tallest waterfall on the planet, albeit underwater. Denmark Strait overflow water in turn eventually contributes to the formation of NADW. It is worth noting that as well as exported deep water, the Arctic also exports cold, very fresh, and therefore light, Polar Water south through both the Canadian Arctic Archipelago and Fram Strait. This light Polar Water has origins in the high Arctic river runoff; net precipitation and sea ice melt mixed with the saltier lower latitude Atlantic and Pacific Waters below.

In the southern hemisphere, the high salinity shelf waters here are exported into the abyssal ocean as AABW (Foster and Carmack, 1976; Orsi et al., 1999). While both the Ross and Weddell Seas are known to be significant sources of high-salinity shelf waters, increasingly, it is thought that AABW is produced all along the Antarctic coastline, rather than in just a few main locations (Gordon, 2009; Williams et al., 2010). Like other water masses of Southern Ocean origin, AABW is spread into the Pacific, Indian, and Atlantic Oceans along the pathway of the ACC and is of particular interest in climate change studies because of the rapidity with which this water mass ventilates so much of our abyssal ocean. Dissolved atmospheric gases and particulate organic carbon entrained in AABW is swiftly transported from the surface to the abyss where it is stored for thousands of years.

The other globally ubiquitous water mass formed in the Southern Ocean is Antarctic intermediate water (AAIW). AAIW is formed as a mode water on the northern edge of the ACC, where Ekman fluxes of fresh polar water across the ACC allow these waters to mix with waters of subtropical gyre character during winter in mixed layers that can easily become 400-m deep (Sloyan et al., 2010; Talley, 1996). Thus AAIW that forms is a very cold and comparatively fresh, eventually subducting below the STMW as it spreads northwards into the Pacific, Atlantic and Indian Oceans (Fig. 2.13).

Temperature and salinity are not just useful in identifying specific water masses, they are also useful for inferring in what proportions two or more water masses have mixed to produce water of intermediate characteristics. For instance, any mixture C of two water masses A and B of given temperature and salinity characteristics will lie on the straight line drawn between the end-member temperature and salinities on a T-S diagram (Fig. 2.6, RHS). The relative proximity of C to either end-member A or B reflects the proportion of each end member in the mix, such that if the A-C distance is three times the C-B distance, then the mixture comprises one-fourth of A and three-fourths of B.

Here we have discussed the main water masses that are found in most ocean basins; however, these water masses are subject to mixing and transformation with regional water masses in their passage through different ocean basins. Different ocean basins are subject to different forcings as a result of their geography and weather systems. For instance, the Mediterranean and, to a lesser degree, the Red Sea both contribute salt to the Atlantic and Indian Oceans, respectively, while the Pacific has no such source of salinity. Hence waters from each of these three basins are easily distinguished by their salt and freshwater content on T-S diagrams.

5. Oceanic impact on and sensitivity to Earth's climate

Geographical differences in water mass formation mechanisms enable the ocean to absorb and store solar radiation at lower latitudes while ventilating the ocean, losing heat to the atmosphere, and forming sea ice at high latitudes. Wind-driven ocean circulation patterns driving warm shallow western boundary currents polewards together with the sinking and equatorwards spread of dense cold bottom waters comprise the global overturning circulation (Fig. 2.14) of our oceans that redistributes heat within the Earth's climate on a global scale. Within the global overturning circulation, water masses transport their properties from formation zones to other

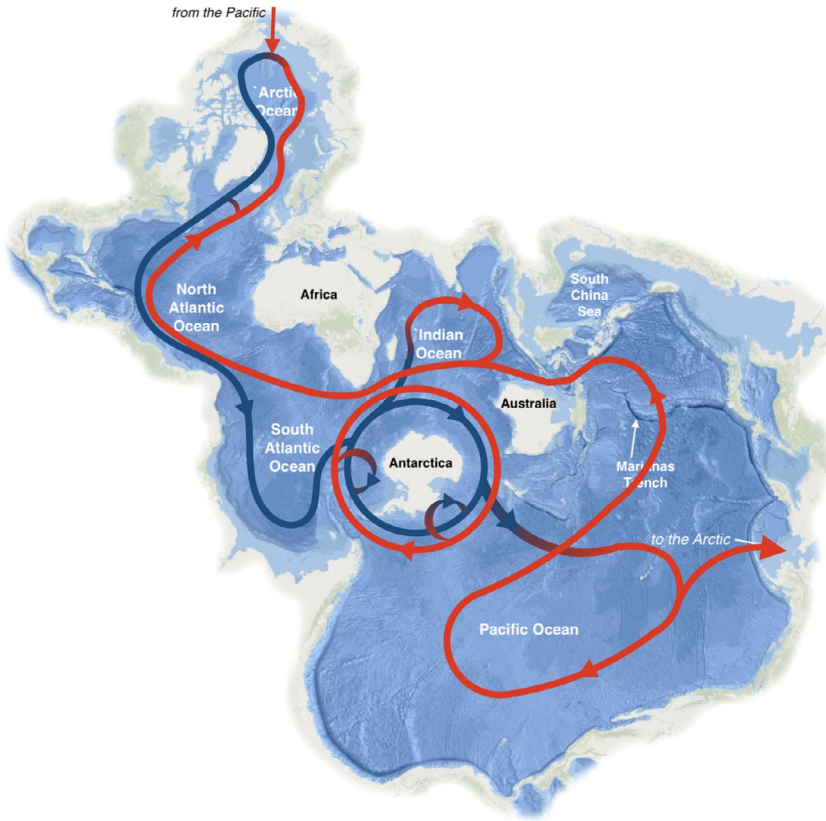

Fig. 2.14 Schematic of the overturning circulation of the global ocean with the warm water pathways depicted in *red* and cool dense water in *blue*.

locations where they are transformed into new water masses either by mixing with ambient waters, air-sea fluxes, or both. Overturning cells within the North Atlantic and Southern Ocean dominate this global thermohaline circulation, with weaker overturning in the Pacific and Indian Oceans completing the loop.

In the North Atlantic, warm water carried in the Gulf Stream eventually feeds into the North Atlantic Current that enters the Iceland Sea before partially recirculating through the Irminger basin, while the remainder follows the European continental slope into the Nordic Seas and the Arctic Ocean. The Gulf Stream/North Atlantic Current forms the surface limb of the North Atlantic's meridional overturning cell (AMOC, Johnson et al., 2019). The warm Gulf Stream water is freshened and cooled in the subpolar

North Atlantic and Arctic basins, ultimately gaining density and being transformed into deep waters that participate in NADW formation. The southward flow of NADW forms the deep return limb of AMOC.

In the Southern Ocean, instead of one overturning cell, there are two. Wind-driven upwelling in the ACC brings isopycnals associated with CDW to the surface at the interface of the two overturning cells. At the surface, some of the upwelled CDW mixes with the fresher polar mixed layer and is fluxed northwards across the ACC by Ekman transport, where it participates in AAIW formation. Together the northward Ekman transport and subducting AAIW form the uppermost limb of the Southern Ocean's overturning cells. The farther south-outcropping CDW isopycnals are transformed by intense winter heat loss and mixing with dense waters of shelf origin to produce AABW that forms the deepest limb of the Southern Ocean's overturning cell.

The transport of ocean heat from low to high latitudes where it can warm the atmosphere makes the climate of these latitudes much milder than if the Earth had no ocean. This exchange of heat and freshwater (through evaporation and precipitation) between the oceans and Earth's atmosphere effectively sets global climate and impacts weather patterns. On longer timescales, the meridional overturning circulation of the oceans supplies oceanic heat to the atmosphere at higher latitudes, making the high-latitude climates more productive and hospitable for life than on a planet without oceans. On shorter timescales of days to weeks, local oceanic hotspots can power storms that absorb both heat and draw water into them through evaporation, such that oceanic hotspots near land can power up tropical storms that wreak devastation on coastlines. The importance of ocean circulation in absorbing, storing, and redistributing heat around the planet cannot be overstated and is a direct result of differences in the density and specific heat capacity, cp, of seawater and the atmosphere.

While scattering and absorption of downwelling solar radiation does occur within the atmosphere, it is largely transparent to visible light which easily passes through and reaches the surface of the planet. Seawater, on the other hand, absorbs visible light, storing this energy as heat, such that heat stored per m^3 for a change in temperature, ΔT, is given as $\Delta Q = \rho_s cp_s \Delta T$, where the s subscript denotes seawater. The specific heat capacity of seawater $cp_s = 3900\,J\,kg^{-1}\,K^{-1}$ and seawater density is typically $1026\,kg\,m^{-3}$, while the density and specific heat capacity of air at 300 K are nominally $1\,kg\,m^{-3}$ and $cp_a = 1000\,J\,kg^{-1}$, respectively. Effectively, the same heat input will change surface air temperature by approximately 4000 times the

temperature change in seawater. This means that as increasing greenhouse gases have trapped more longwave radiation, the oceans have been critical for keeping the planet cool, as measurements and historical reconstructions show that the oceans have absorbed about 90% of the excess heat (Cheng et al., 2020; Zanna et al., 2019).

Yet this increased ocean heat storage has already had an impact on life on the planet. First, the oceans have expanded as they warmed, contributing to sea level rise (Domingues et al., 2008; Levitus et al., 2012). Sea level rise has accelerated coastal erosion, threatened salt marshes, will reconfigure barrier islands (FitzGerald et al., 2008; Neumann et al., 2015), and is inundating low-lying islands at a rate that threatens the medium-term existence of several island nations. Second, warmer ocean temperatures have resulted in an increasing frequency of coral bleaching events (Glynn, 1991; van Hooidonk et al., 2016; Hughes et al., 2017) that purges corals of their symbiotic zooxanthellae, imperiling the survival of many reefs and changing their ecosystems (Hughes et al., 2018). Third, rising temperatures reduce the solubility of gasses in the ocean, including oxygen which is critical for respiration. Indeed, the reduction in oxygen concentration levels in many regions of the ocean has already been documented (Breitburg et al., 2018; Shaffer et al., 2009), with numerical models predicting future dire consequences for phytoplankton that are the primary producers of the ocean (Sekerci and Petrovskii, 2015; see also Chapter 13). Any decrease in ocean primary production, in turn, reduces the ocean's ability to fix atmospheric carbon dioxide and sequester it from the atmosphere and, in other words, reducing the ocean's role as a critical store for atmospheric carbon dioxide. Finally, the warming ocean's impact on Arctic sea ice has been increasing in the last few decades (Barton et al., 2018; Lind et al., 2018; Polyakov et al., 2020), contributing to the loss in seasonal sea ice and reducing the earth's albedo with consequences for marine ecosystems and the planetary energy budget. Oceanic warmth is also undermining tidewater glaciers in Greenland (Millan et al., 2018; Rignot et al., 2016; Wood et al., 2018) and ice shelves in Antarctica (DeConto and Pollard, 2016; Jacobs et al., 1979; Rignot et al., 2013; Stanton et al., 2013). The consequence of this melting is to accelerate the glacier streams toward the ocean, enhancing the contribution of land-based ice to sea level rise.

Clearly, on multiple timescales from days to decades, how the ocean transports heat, freshwater, and other tracers around the globe has profound consequences for our planet. And although proper energetics of ocean circulation is still an ongoing discussion, it is evident that tides and the energy

they dissipate drive ocean mixing and mediates the transfer of heat between oceanic layers, and the atmosphere, in different ways that impacts the global overturning circulation both today and throughout Earth's history (Green et al., 2009; Schmittner et al., 2015; Wilmes et al., 2021). Thus no story of our oceans would be complete without a focus on tides.

Acknowledgments

The authors acknowledge the following funding for this contribution: YDL, the UK-German NERC-BMBF Changing Arctic Ocean PEANUTS project (NE/R01275X/1), and NERC ArctiCONNECT consortium NE/V005855/1. The ARMOR3D hydrographic product can be found at https://doi.org/10.48670/moi-00052. EN.4.2.2 data were obtained from https://www.metoffice.gov.uk/hadobs/en4/ and are © British Crown Copyright, Met Office, provided under a Non-Commercial Government License http://www.nationalarchives.gov.uk/doc/non-commercial-government-licence/version/2/.

References

Adcroft, A., Scott, J.R., Marotzke, J., 2001. Impact of geothermal heating on the global ocean circulation. Geophys. Res. Lett. 28 (9). https://doi.org/10.1029/2000GL012182.

Barton, B.I., Lenn, Y.D., Lique, C., 2018. Observed Atlantification of the Barents Sea causes the polar front to limit the expansion of winter sea ice. J. Phys. Oceanogr. 48, 1849–1866. https://doi.org/10.1175/JPO-D-18-0003.1.

Beal, L.M., Bryden, H.L., 1999. The velocity and vorticity structure of the Agulhas Current at 32 S. J. Geophys. Res. Oceans 104 (C3), 5151–5176.

Boyle, R., 1685. Short memoirs for the natural experimental history of mineral waters: by the Honourable Robert Boyle, Fellow of the Royal Society. London. 1685; Octavo. Philos. Trans. R. Soc. 15 (172), 1063–1066.

Breitburg, D., Levin, L.A., Oschlies, A., Grégoire, M., Chavez, F.P., Conley, D.J., et al., 2018. Declining oxygen in the global ocean and coastal waters. Science 359 (6371), eaam7240.

Cheng, L., Abraham, J., Zhu, J., Trenberth, K.E., Fasullo, J., Boyer, T., Locarnini, R., et al., 2020. Record-setting ocean warmth continued in 2019. Adv. Atmos. Sci. 37, 137–142.

Clarke, R.A., Gascard, J.-C., 1983. The formation of Labrador Sea water. Part I: large-scale processes. J. Phys. Oceanogr. 13 (10), 1764–1778.

DeConto, R.M., Pollard, D., 2016. Contribution of Antarctica to past and future sea-level rise. Nature 531, 591–597. https://doi.org/10.1038/nature17145.

Domingues, C.M., Church, J.A., White, N.J., Gleckler, P.J., Wijffels, S.E., Barker, P.M., Dunn, J.R., 2008. Improved estimates of upper-ocean warming and multi-decadal sea-level rise. Nature 453, 1090–1093. https://doi.org/10.1038/nature07080.

FitzGerald, D.M., Fenster, M.S., Argow, B.A., Buynevich, I.V., 2008. Coastal impacts due to sea-level rise. Annu. Rev. Earth Planet. Sci. 36, 601–647.

Foster, T.D., Carmack, E.C., 1976. Frontal zone mixing and Antarctic bottom water formation in the Southern Weddell Sea. In: Deep Sea Research and Oceanographic Abstracts. Elsevier.

Friedlingstein, P., et al., 2020. Global carbon budget 2020. Earth Syst. Sci. Data 12 (4). https://doi.org/10.5194/essd-12-3269-2020.

Glorioso, P.D., Simpson, J.H., 1994. Numerical modelling of the M2 tide on the northern Patagonian shelf. Cont. Shelf Res. 14 (2/3), 267–278. https://doi.org/10.1016/0278-4343(94)90016-7.
Glynn, P.W., 1991. Coral reef bleaching in the 1980s and possible connections with global warming. Trends Ecol. Evol. 6 (6), 175–179.
Good, S.A., Martin, M.J., Rayner, N.A., 2013. EN4: quality controlled ocean temperature and salinity profiles and monthly objective analyses with uncertainty estimates. J. Geophys. Res. Oceans 118, 6704–6716.
Gordon, A.L., 2009. Bottom water formation. In: Ocean Currents. vol. 263. Associated Press, New York, NY, p. 269.
Green, J.A.M., Schmittner, A., 2015. Climatic consequences of a Pine Island glacier collapse. J. Climate 28 (23), 9221–9234. https://doi.org/10.1175/JCLI-D-15-0110.1.
Green, J.M., Green, C.L., Bigg, G.R., Rippeth, T.P., Scourse, J.D., Uehara, K., 2009. Tidal mixing and the meridional overturning circulation from the last glacial maximum. Geophys. Res. Lett. 36 (15). https://doi.org/10.1029/2009GL039309.
Grumbine, R.W., 1991. A model of the formation of high-salinity shelf water on polar continental shelves. J. Geophys. Res. Oceans 96 (C12), 22049–22062.
Guinehut, S., Dhomps, A.-L., Larnicol, G., Le Traon, P.-Y., 2012. High resolution 3-d temperature and salinity fields derived from in situ and satellite observation. Ocean Sci. 8, 845–857. https://doi.org/10.5194/os-8-845-2012).
Hoffmann, J., Wilmsmeier, G., Lun, Y.H.V., 2017. Connecting the world through global shipping networks. J. Ship. Trade 2, 2.
Horner-Devine, A.R., Hetland, R.D., MacDonald, D.G., 2015. Mixing and transport in coastal river plumes. Annu. Rev. Fluid Mech. 47 (47), 569–594. https://doi.org/10.1146/annurev-fluid-010313-141408.
Hughes, T.P., Kerry, J.T., Álvarez-Noriega, M., Álvarez-Romero, J.G., Anderson, K.D., Baird, A.H., et al., 2017. Global warming and recurrent mass bleaching of corals. Nature 543 (7645), 373–377.
Hughes, T.P., Anderson, K.D., Connolly, S.R., Heron, S.F., Kerry, J.T., Lough, J.M., et al., 2018. Spatial and temporal patterns of mass bleaching of corals in the Anthropocene. Science 359 (6371), 80–83.
Huthnance, J., 1984. Slope currents and 'JEBAR'. J. Phys. Oceanogr. 14 (4), 795–810.
Jacobs, S.S., Gordon, A.L., Ardai, J., 1979. Circulation and melting beneath the Ross Ice Shelf. Science 203 (4379), 439–443.
Johnson, H.L., Cessi, P., Marshall, D.P., Schloesser, F., Spall, M.A., 2019. Recent contributions of theory to our understanding of the Atlantic meridional overturning circulation. J. Geophys. Res. Oceans 124, 5376–5399. https://doi.org/10.1029/2019JC015330.
Knudsen, M., 1900. Ein hydrographischer lehrsatz. Ann. Hydrogr. Marit. Meteorol. 28 (7), 316–320.
Lake, R., Lewis, E., 1970. Salt rejection by sea ice during growth. J. Geophys. Res. 75 (3), 583–597.
Lammers, R.B., et al., 2001. Assessment of contemporary Arctic river runoff based on observational discharge records. J. Geophys. Res. Atmos. 106 (D4), 3321–3334.
Levitus, S., et al., 2012. World Ocean heat content and thermosteric sea level change (0–2000 m), 1955–2010. Geophys. Res. Lett. 39, L10603. https://doi.org/10.1029/2012GL051106.
Lilly, J.M., et al., 1999. Observing deep convection in the Labrador Sea during winter 1994/95. J. Phys. Oceanogr. 29 (8), 2065–2098.
Lind, S., Ingvaldsen, R.B., Furevik, T., 2018. Arctic warming hotspot in the northern Barents Sea linked to declining sea-ice import. Nat. Clim. Chang. 8 (7), 634–639.
McCartney, M.S., Talley, L.D., 1982. The subpolar mode water of the North Atlantic Ocean. J. Phys. Oceanogr. 12, 1169–1188.

Millan, R., Rignot, E., Mouginot, J., Wood, M., Bjørk, A.A., Morlighem, M., 2018. Vulnerability of Southeast Greenland glaciers to warm Atlantic water from operation icebridge and ocean melting Greenland data. Geophys. Res. Lett. 45 (6), 2688–2696.
Nehama, F.P.J., Reason, C.J.C., 2021. Modelling the Zambezi River plume. Afr. J. Mar. Sci. 37, 593–604. https://doi.org/10.2989/1814232X.2015.1113202.
Neumann, B., et al., 2015. Future coastal population growth and exposure to sea-level rise and coastal flooding—a global assessment. PLoS One 10 (3). https://doi.org/10.1371/journal.pone.0118571.
Niedrauer, T.M., Martin, S., 1979. An experimental study of brine drainage and convection in young sea ice. J. Geophys. Res. Oceans 84 (C3), 1176–1186.
Orsi, A.H., Johnson, G.C., Bullister, J.L., 1999. Circulation, mixing, and production of Antarctic bottom water. Prog. Oceanogr. 43 (1), 55–109.
Park, H., et al., 2020. Increasing riverine heat influx triggers Arctic sea ice decline and oceanic and atmospheric warming. Sci. Adv. 6 (45). https://doi.org/10.1126/sciadv.abc4699.
Polton, J.A., 2015. Tidally induced mean flow over bathymetric features: a contemporary challenge for high-resolution wide-area models. Geophys. Astrophys. Fluid Dyn. 109 (3), 207–215.
Polyakov, I.V., Alkire, M.B., Bluhm, B.A., Brown, K.A., Carmack, E.C., Chierici, M., et al., 2020. Borealization of the Arctic Ocean in response to anomalous advection from sub-Arctic seas. Front. Mar. Sci. 7, 491.
Pritchard, D.W., 1956. The dynamic structure of a coastal plain estuary. J. Mar. Res. 15 (1), 33–42.
Raiswell, R., et al., 2008. Bioavailable iron in the Southern Ocean: the significance of the iceberg conveyor belt. Geochem. Trans. 9 (1), 1–9.
Reid, J.L., 1979. On the contribution of the Mediterranean Sea outflow to the Norwegian-Greenland Sea. Deep Sea Res. Part A. Oceanogr. Res. Pap. 26 (11), 1199–1223.
Rignot, E., Jacobs, S., Mouginot, J., Scheuchl, B., 2013. Ice-shelf melting around Antarctica. Science 341 (6143), 266–270.
Rignot, E., Xu, Y., Menemenlis, D., Mouginot, J., Scheuchl, B., Li, X., et al., 2016. Modeling of ocean-induced ice melt rates of five west Greenland glaciers over the past two decades. Geophys. Res. Lett. 43 (12), 6374–6382.
Rippeth, T.P., 2005. Mixing in seasonally stratified shelf seas: a shifting paradigm. Philos. Trans. Royal Soc. A: Math. Phys. Eng. Sci. 363 (1837), 2837–2854.
Rudels, B., et al., 2005. The interaction between waters from the Arctic Ocean and the Nordic Seas north of Fram Strait and along the East Greenland current: results from the Arctic Ocean-02 oden expedition. J. Mar. Syst. 55 (1–2), 1–30.
Scales, H., 2021. The Brilliant Abyss. Bloomsbury Publishing.
Schauer, U., 1995. The release of brine-enriched shelf water from Storfjord into the Norwegian Sea. J. Geophys. Res. Oceans 100 (C8), 16015–16028.
Schmittner, A., Green, J.A.M., Wilmes, S.B., 2015. Glacial Ocean overturning intensified by tidal mixing in a global circulation model. Geophys. Res. Lett. 42 (10), 4014–4022.
Schott, F., Visbeck, M., Send, U., 1994. Open ocean deep convection, Mediterranean and Greenland Seas. In: Ocean Processes in Climate Dynamics: Global and Mediterranean Examples. Springer, pp. 203–225.
Sekerci, Y., Petrovskii, S., 2015. Mathematical modelling of plankton–oxygen dynamics under the climate change. Bull. Math. Biol. 77 (12), 2325–2353.
Shaffer, G., Olsen, S.M., Pedersen, J.O.P., 2009. Long-term ocean oxygen depletion in response to carbon dioxide emissions from fossil fuels. Nat. Geosci. 2 (2), 105–109.
Sharples, J., Simpson, J.H., 1993. Periodic frontogenesis in a region of freshwater influence. Estuaries 16 (1), 74–82.
Silva, T., Bigg, G., Nicholls, K., 2006. Contribution of giant icebergs to the Southern Ocean freshwater flux. J. Geophys. Res. Oceans 111 (C3). https://doi.org/10.1029/2004JC002843.

Simpson, J.H., et al., 1990. Tidal straining, density currents, and stirring in the control of estuarine stratification. Estuaries 13 (2), 125–132.
Simpson, J.H., et al., 1996. The vertical structure of turbulent dissipation in shelf seas. J. Phys. Oceanogr. 26 (8), 1579–1590.
Sloyan, B.M., et al., 2010. Antarctic intermediate water and subantarctic mode water formation in the Southeast Pacific: the role of turbulent mixing. J. Phys. Oceanogr. 40 (7), 1558–1574.
Small, C., Nicholls, R.J., 2003. A global analysis of human settlement in coastal zones. J. Coast. Res. 19 (3), 584–599.
Speer, K., Rintoul, S.R., Sloyan, B., 2000. The diabatic deacon cell. J. Phys. Oceanogr. 30 (12), 3212–3222.
Stanton, T.P., Shaw, W.J., Truffer, M., Corr, H.F.J., Peters, L.E., Riverman, K.L., et al., 2013. Channelized ice melting in the ocean boundary layer beneath Pine Island Glacier. Antarct. Sci. 341 (6151), 1236–1239.
Stommel, H., 1948. The westward intensification of wind-driven ocean currents. Eos 29 (2), 202–206.
Stramma, L., Ikeda, Y., Peterson, R.G., 1990. Geostrophic transport in the Brazil Current region north of 20 S. Deep Sea Res. Part A. Oceanogr. Res. Pap. 37 (12), 1875–1886.
Sverdrup, H.U., 1947. Wind-driven currents in a baroclinic ocean; with application to the equatorial currents of the Eastern Pacific. Proc. Natl. Acad. Sci. U. S. A. 33 (11), 318–326.
Talley, L., 1996. Antarctic intermediate water in the South Atlantic. In: The South Atlantic. Springer, pp. 219–238.
Talley, L.D., Pickard, G.E., Emery, W.J., Swift, J.H., 2011. Descriptive Physical Oceanography: An Introduction, sixth ed. Elsevier, Burlington, MA, p. 560.
Thomas, H., et al., 2004. Enhanced open ocean storage of CO_2 from shelf sea pumping. Science 304 (5673), 1005–1008.
Tsunogai, S., Watanabe, S., Sato, T., 1999. Is there a 'continental shelf pump' for the absorption of atmospheric CO_2? Tellus B Chem. Phys. Meteorol. 51 (3), 701–712.
Van Hooidonk, R., Maynard, J., Tamelander, J., Gove, J., Ahmadia, G., Raymundo, L., Williams, G., Heron, S.F., Planes, S., 2016. Local-scale projections of coral reef futures and implications of the Paris Agreement. Sci. Rep. 6, 1–8. https://doi.org/10.1038/srep39666.
Verne, J., 1869. Vingt mille lieues sous les mers. Pierre-Jules Hetzel.
Wettlaufer, J., Worster, M.G., Huppert, H.E., 1997. The phase evolution of young sea ice. Geophys. Res. Lett. 24 (10), 1251–1254.
Williams, G.D., Aoki, S., Jacobs, S.S., Rintoul, S.R., Tamura, T., Bindoff, N.L., 2010. Antarctic bottom water from the Adélie and George V Land coast, East Antarctica (140–149 E). J. Geophys. Res. Oceans 115 (C4). https://doi.org/10.1029/2009JC005812.
Wilmes, S.-.B., Green, J.A., Schmittner, A., 2021. Enhanced vertical mixing in the glacial ocean inferred from sedimentary carbon isotopes. Commun. Earth Environ. 2 (1), 1–9.
Wood, M., Rignot, E., Fenty, I., Menemenlis, D., Millan, R., Morlighem, M., et al., 2018. Ocean-induced melt triggers glacier retreat in Northwest Greenland. Geophys. Res. Lett. 45 (16), 8334–8342.
Worthington, L., 1958. The 18 water in the Sargasso Sea. Deep Sea Research (1953) 5 (2–4), 297–305.
Zanna, L., Khatiwala, S., Gregory, J.M., Ison, J., Heimbach, P., 2019. Global reconstruction of historical ocean heat storage and transport. Proc. Natl. Acad. Sci. U. S. A. 116, 1126–1131. https://doi.org/10.1073/pnas.1808838115.